Topology of HI Gas Distribution in the Large Magellanic Cloud

Sungeun Kim[1] and Changbom Park[2]

ABSTRACT

We have analyzed the H I aperture synthesis image of the Large Magellanic Cloud (LMC), using an objective and quantitative measure of topology to understand the H I distribution hosting a number of holes and clumps of various sizes in the medium. The H I distribution shows different topology at four different chosen scales. At the smallest scales explored ($19 \sim 29$ pc), the H I mass is distributed in such a way that numerous clumps are embedded on top of a low density background. At the larger scales from 73 to 194 pc, it shows a generic hole topology. These holes might have been formed mainly by stellar winds from hot stars. At the scales from 240 to 340 pc, slightly above the disk scale-height of the gaseous disk, major clumps in the H I map change the distribution to have a slight clump topology. These clumps include the giant cloud associations in the spiral arms and the thick filaments surrounding superholes. At the largest scales studied ($390 \sim 485$ pc), the hole topology is present again. Responsible to the hole topology at this scale are a few superholes which seem mainly associated with supernova explosions in the outer disk. The gaps between the bar and spiral arms have a minor effect on the topology at this scale.

Subject headings: galaxies: individual (Large Magellanic Cloud) — galaxies: ISM — ISM: neutral hydrogen — Magellanic Clouds — radio lines: HI

1. Introduction

The topology of the interstellar medium (ISM) is critical in understanding the nature of the underlying physical structure that gives us the observed spatial and velocity structures. The global structure of the ISM is manifested by the spatial and velocity structures of the neutral hydrogen gas. Atomic hydrogen is known to be an important component of the

[1]Astronomy & Space Science Department, Sejong University, 98 Kwangjin-gu, Seoul 143-747, Korea; Email: sek@sejong.ac.kr

[2]Korea Institute for Advanced Study, Dongdaemun-gu, Seoul 130-722, Korea

ISM (Burton 1992). Relatively high-resolution H I images of nearby galaxies obtained with radio aperture synthesis interferometers have shown overall clumpy H I distributions and various structures such as holes, shells, loops, filaments, and bubbles (Brinks and Bajaja 1986; Deul and den Hartog 1990; Kamphuis, Sancisi, and van der Hulst 1991; Puche et al. 1992; Staveley-Smith et al. 1997; Kim et al. 1998; Stanimirovic et al. 1999; Thilker et al. 2000; Walter and Brinks 2001).

One of the most striking results of these surveys is that the H I supergiant shells (SGSs) occupy a large volume of the ISM as such the H I filaments seen in the Galaxy (Heiles 1984). About twenty SGSs with their diameters larger than 750 pc are identified in the Large Magellanic Cloud (LMC), of which 1/3 are associated with optical counterparts detected in the Hα emission (Kim et al. 1999). Many of these H I shells are found in regions of very active star formation in the LMC. Massive stars interact with the ambient ISM through fast stellar winds and supernovae ejecta to form interstellar shell structures with sizes ranging from 10 pc to greater than 1000 pc. However, the correlation between the H I shells and 122 OB stellar associations in the LMC (Lucke and Hodge 1970) is not very tight. No star clusters were found at the center of the H I holes in Holmberg II (Rhode et al. 1999) and the Galaxy (Heiles 1984). Deul and den Hartog (1990) have reported that the H I holes larger than 500 pc are in general located at the interarm cavities and not likely to be produced by the H II regions and OB associations. The energy required to produce such an H I hole is at least 10^{53} ergs (Kamphuis et al. 1991). These observations have risen an interesting question about the origin of these structures and whether these H I holes have been formed by the interaction between massive stars and the ISM or not. In fact, high-resolution two-dimensional hydrodynamical simulations present that the large cavities of the ISM may be formed by the nonlinear development of the combined thermal and gravitational instabilities, without need for stellar energy injection in a galaxy modeling of the LMC (Wada et al. 2000). In their study, dense clumps and filamentary structures are formed as a natural consequence of the nonlinear evolution of the multiphase ISM.

In this paper, we present a method to disentangle the character of the structures seen in the H I distribution in the LMC as a function of scale using the genus statistic. We find that the genus curve can give information on the shape and topological properties of H I structure at different scales. The relationship between the amplitude of the genus curve and the slope of the power spectrum has been investigated in the current paper.

2. Observational Data

We use an H I aperture synthesis image from the high resolution HI survey of the LMC with the Australia Telescope Compact Array (ATCA) at 1421 MHz with velocity coverage from −33 to 627 km/s (Kim et al. 1998). The results of H I aperture synthesis mosaic of the LMC were made by combining data from 1344 separate pointing centers and correspond to $11^{\circ}.1 \times 12^{\circ}.4$ on the sky. We have produced an HI brightness temperature map of the LMC from the brightest H I component at each position. The spatial resolution of the map is $50'' \sim 55''$ corresponding to 12∼14 pc at the LMCs distance of 50.1 kpc (Alves 2004). At which, the LMC can be mapped with a high spatial resolution and both the interstellar structures and their underlying stars can be resolved and examined in great detail. Having low inclination angles, the LMC can be studied with little confusion along the line-of-sight. With small foreground and internal extinctions, the LMC can be easily observed at UV and X-ray wavelengths. The pixel size of the synthesis map is $20''$. Figure 1 shows the resulting HI map of the LMC. The lines are circles of radii of 700, 600, and 500 pixels (from outside to inward). We mainly choose to analyze the region within the circle of radius of 600 pixels ($200'$ or 3.0 kpc). This region contains most of the interesting structures and is not much affected by the outer edge of the disk.

3. The Genus Statistic

We use the genus statistic to quantify the geometric shape of the projected HI distribution of the LMC. The intrinsic topology of iso-temperature or iso-density contours can be measured by the genus. The genus of an object has a meaning of the largest number of cuts that can be made through it without dividing it into two pieces. Following Melott et al. (1989) and Gott et al. (1990) we adopt, for repeatedly or infinite connected contours in the plane, a modified definition of the two-dimensional genus

$$G(\nu) = \#\text{ of isolated high density regions} - \#\text{ of low density holes.} \quad (1)$$

This genus equals to 1 minus the mathematically-defined genus. For example, the genus of a ring will be zero because it has one connected high density region and one hole. On the other hand, the genus of a disk is plus one because it has one isolated high density region and no hole. In the case of the HI map of the LMC we first smooth the map over a scale we are interested in, and construct the iso-density contours at a set of threshold levels. The genus is then calculated by integrating the local curvature along the contours. With a threshold

level ν the mathematical form of the genus is

$$G(\nu) = \frac{1}{2\pi} \sum_i \oint_{C_i} \kappa ds, \tag{2}$$

where κ is the local (signed) curvature on an isodensity contour C_i. We define the sign of κ so that it is positive when a contour encloses a high density region counterclockwise (Gott et al. 1990; Park et al. 1992; Park, Gott, & Choi 2001). A genus curve is obtained by measuring the genus at a set of threshold levels. A good feature of the genus statistic is that the analytic formula of the genus curve is known for a Gaussian random field. The genus for a Gaussian random phase field is

$$g(\nu) = A\nu e^{-\nu^2/2}, \tag{3}$$

where the amplitude A depends only on the shape of the power spectrum of the field but not on its amplitude (see eqs. 8 and 9). Any deviation of a measured genus curve from this formula is evidence for non-Gaussianity, and reveals the nature of the geometrical shape of the fluctuation. The threshold levels are chosen so that they can represent area fractions. A threshold level with a label ν corresponds to the area fraction

$$f_\nu = \frac{1}{(2\pi)^{1/2}} \int_\nu^\infty e^{-x^2/2} dx. \tag{4}$$

Contours with $\nu = 1.0, 0.0$, and -1.0 enclose 16, 50, and 84% of the total area, respectively.

To get an idea of what the genus curve indicates about the shape of structures in the disk of a galaxy, we show in Figure 2 the genus curves of three toy models. The solid line is the genus curve of a disk filled with randomly fluctuating but statistically uniform matter smoothed over $\lambda_{\rm FWHM} = 2'$ by a Gaussian filter. This Poission matter fluctuation yields a Gaussian random field, and the genus curve has the form of equation (3). The dashed line with filled circles is for a uniform disk with additional 857 randomly distributed clumps of diameter of $4'$. In this case of clump topology, the genus curve is shifted to the left, and becomes asymmetric. The dotted line with open circles is for a uniform disk with 857 randomly distributed empty holes of diameter of $4'$. The genus curve is now shifted to the right and also becomes asymmetric, indicating that the shape of the low density regions is altered by the holes. Since the area fraction is fixed at a given ν, the low amplitude of the genus curve means fewer number of structures with bigger size compared to the expectation for a Gaussian field. Therefore, the genus curve tells not only the deviation of a field from the Gaussian one, but also the statistical nature of the field too. Even though the true nature of the HI distribution in the LMC is three dimensional, the projected view of the distribution shown in Figure 1 reveals a wealth of interesting structures, which deserve a two dimensional

topology study. The two dimensional genus statistic has been applied to the distribution of galaxies when the data is the projected distribution of galaxies on the sky or the distribution of galaxies in a thin slice (Melott et al. 1989; Park et al. 1992).

4. Results

To measure the genus we smooth the HI image of the LMC and cut the circular area of the disk within $200'$ from the center. The genus curves of the HI distribution of the LMC for 12 selected smoothing scales are shown in Figure 3. In each panel three genus curves are plotted and their Gaussian smoothing lengths are denoted in units of arcminutes. The solid line in each panel is the Gaussian curve (eq. 3) best fit to the filled circles corresponding to the median smoothing length. Open circles represent the shortest smoothing length. The genus curve for $\lambda_{\rm FWHM} = 1.7'$ (open circles in the lower right panel) smoothing shows no shift, but the negative side has an amplitude higher than the positive side. This means that the low density regions are broken into numerous pieces while the high density regions are relatively more connected into fewer number of pieces at the same volume fraction. Therefore, the genus curve indicates that there are coherent high density clumps distributed on a noisy (low fluctuation amplitude) background at this shortest scale. On the other hand, the genus curves corresponding to $\lambda_{\rm FWHM} = 10'$ or $13'$ (filled circles or squares in the lower left panel) shows a slight shift to the right and the low density part has a lower amplitude. This is a generic shape of a hole topology as shown in Figure 2. At larger smoothing lengths the genus curves become noisier and the topological structure of the HI disk is not obvious from Figure 3.

To make more quantitative measurements of the shift and asymmetry of the genus curve, we develop pseudo-statistics derived from the genus curve. We first find the best-fit amplitude of the Gaussian genus curve for each measured genus curve over the interval $-2 \leq \nu \leq +2$. We quantify the shift by

$$\Delta\nu = \int_{-1}^{1} \nu G(\nu) d\nu / \int_{-1}^{1} G_G(\nu) d\nu, \tag{5}$$

where G_G is the best-fit Gaussian genus curve (Park et al. 2001). The asymmetry of the genus curve at high density levels is quantified by

$$A_C = \int_{0.7}^{2} G(\nu) d\nu / \int_{0.7}^{2} G_G(\nu) d\nu. \tag{6}$$

If the measured genus is lower than the best-fit Gaussian curve at high threshold levels, the parameter A_C will be less than 1, meaning that the high density regions are more connected

into fewer larger pieces compared to the Gaussian case. The asymmetry parameter A_H at low density levels is similarly defined with the integration interval from -0.7 to -2.0,

$$A_H = \int_{-2}^{-0.7} G(\nu)d\nu / \int_{-2}^{-0.7} G_G(\nu)d\nu. \quad (7)$$

If the low density regions are well-connected to one another or dominated by a few large holes, the genus becomes lower than Gaussian expectation and the parameter A_H becomes less than 1.

Figure 4 shows interesting variations of the shift and asymmetry parameters as functions of smoothing scale. The circles and triangles in the upper panel are the shift parameters measured from the circular areas with radii of $200'$ and $167'$, respectively. The difference between the two cases is a measure of the uncertainty in the shift parameter. They show that the results are generally robust against the choice of the outer boundary. In the bottom panel the asymmetry parameters A_C (filled circles) and A_H are plotted. These parameters reveal an interesting change of topology as the scale changes. At the smallest scales studied ($1.3' \sim 2'$ or $19 \sim 29$ pc), the shift parameter is nearly zero while $A_C < 1$ and $A_H > 1$, which was seen in the lower right panel of Figure 3. This corresponds to the situation when there are clumps embedded in the background HI distribution which has low-amplitude random fluctuations. At high density thresholds the clumps are detected and their number density falls below that of Gaussian random field. But at low thresholds the isolated low density holes are found in the fluctuating background, and their number density exceeds that of the best-fit Gaussian model.

At the next larger scales ($5' \sim 13'$ or $73 \sim 194$ pc) the HI map shows a generic hole topology. The shift parameter is positive, and the genus curve is asymmetric in the sense that the low density holes are fewer (or larger in size) than the Gaussian expectation. This was also noticed in the lower left panel of Figure 3. The transition from the clump to the hole topology occurs at about $3'$ or 48 pc. At the still larger scales of $17' \sim 23'$ or $240 \sim 340$ pc the asymmetry of the genus curve remains the same, but the shift parameter suddenly drops to slightly negative values. The clump topology is not statistically significant when the uncertainty at these scales is taken into account, but the change in topology is clear. It seems that there are large dense clumps as well as large holes of similar sizes at these scales. The large clumps are large enough to show up in the shift parameter, but are not prominent and numerous enough to change the whole topology of the disk. The scale is about 1/10 of the size of disk, and the corresponding clumps are mainly distributed along the bar and spirals arms. Some of them are filaments around the biggest holes.

At the largest scales explored ($27' \sim 33'$ or $390 \sim 485$ pc) the genus curves are very noisy because of the small number of resolution elements at these large smoothing scales.

However, the genus-related parameters suggest a hole topology at these scales. The shift parameter, though uncertain, is positive, and the genus curve is asymmetric again with low amplitude at low density thresholds as in the second case above. There are a few big holes causing this behavior of the genus curve. They are mainly the roughly circular giant holes in the upper left part of the disk rather than the gaps between spiral arms (see Figure 1). The lower right part, where there are several connected holes of smaller sizes located between the spiral arms, also contributes to the hole shift.

In addition to the topology of the H I distribution we also study its power spectrum because the characteristic scales showing topological changes could appear in the shape of power spectrum as well. The amplitude of the genus curve can be used to explore the slope of the power spectrum near the smoothing scale. Consider a two dimensional Gaussian random field, whose power spectrum is $P(k)$, which is smoothed by a Gaussian kernel $F(k) = \exp(-k^2 R_G^2/2)$ over a smoothing length R_G. Then the genus curve per unit area in equation (2) is given by

$$A = \frac{1}{(2\pi)^{3/2}} \frac{\langle k^2 \rangle}{2}, \tag{8}$$

where

$$\langle k^2 \rangle = \int k^2 P(k) F^2(k) dk / \int P(k) F^2(k) dk. \tag{9}$$

When the power spectrum is a power-law one, $P(k) \propto k^n$, the moment of power spectrum is given by

$$\langle k^2 \rangle = (n_{\rm eff} + 2)/2R_G^2. \tag{10}$$

Note that the Gaussian smoothing length is related with the FWHM by $\lambda_{\rm FWHM} = 2\sqrt{2\ln 2} R_G$. For Poission noise $n = 0$, and the total genus at $\nu = 1$ is expected to be 3350 for an area with radius of $200'$ and a smoothing scale of $\lambda_{\rm FWHM} = 2'$. This is exactly what is seen for the random mass distribution in Figure 2 (solid curve).

The upper panel of Figure 5 shows the amplitude of the genus curve per unit square degree as a function of the smoothing scale. For a Gaussian matter fluctuation with a perfect power-law power spectrum it will scale as λ^{-2}. But it is dropping faster than that at larger scales. The bottom panel shows the effective power index of the power spectrum at the smoothing scale calculated from equation (10) assuming that the HI distribution is a Gaussian random field. Even though the HI distribution is not exactly Gaussian, the deviation is not great as can be seen in Figures 3 and 4 and the index of the power spectrum measured by eq. (10) can serve as an estimate of the true index. Figure 5 shows that the power index continuously increases from the smallest scale studied to about $\lambda_{\rm FWHM} = 20'$, where it stays more or less constant at -1. The $20'$ scale is where the clump and hole topologies are competing with each other. The power index of -1.8 at the smallest scale

means that the HI mass fluctuation is nearly scale-free. On the other hand, $n \gg -2$ at larger scales means that the mass fluctuation is higher at small scales and lower at large scales. The constancy of the power index at scales larger than $20'$ might mean there is some mechanism generating additional matter fluctuations at those scales and above.

5. Discussion

We performed a topological analysis of the H I map of the LMC which hosts a number of holes and clumps of various sizes. The H I distribution shows different topology at four different scales. At the smallest scale explored ($19 \sim 29$ pc) the H I mass is distributed in such a way that numerous clumps are embedded on top of a low density background. At the larger scales from 73 to 194 pc it shows a generic hole topology. These holes might have been mainly formed by stellar wind from massive stars and SNe. Therefore, the structure of the neutral atomic interstellar gas is dominated by numerous small clumps and relatively larger holes at the scales less than the scale-height of the gaseous disk, which has been estimated to be approximatedly 180 pc (Kim et al. 1999).

At the scales from 240 to 340 pc major clumps in the H I map change the distribution to a slight clump topology. These H I clumps include the giant cloud associations in the spiral arms and the thick filaments surrounding large holes. At the largest scales studied ($390 \sim 485$ pc) the hole topology is again detected. Responsible to the hole topology are a few large holes which seem mainly associated with supernova explosions at outer disk. The gaps between the bar and spiral arms have minor effects.

We have also measured the effective power index of the power spectrum of the H I map. The H I distribution has a nearly scale-free power spectrum at the smallest scales explored. But the power index continuously increases at larger scales. This means that the H I mass fluctuation at these scales is dominated by the power at smaller scales. At scales larger than 290 pc the power index stays at a roughly constant value of -1.05 ± 0.05. This transition scale is comparable to the H I scale-height estimated from the average vertical velocity dispersion and the average surface density of both the H I and the stellar components of the LMC disk (Kim et al. 1999). However, a wavelength of 290 pc is still shorter than the warm H I diffuse layer having a thickness of 350 pc estimated from the basis of supershell model for LMC 2 (Wang & Helfand 1991).

We thank Yun-Young Choi for her help for illustration. SK and CBP acknowledge the support of the Korea Science and Engineering Foundation (KOSEF) through the Astrophysical Research Center for the Structure and Evolution of the Cosmos (ARCSEC).

REFERENCES

Alves, D.R. 2004, NewAR., 48, 659

Brinks, E. & Bajaja, E. 1986, A&A, 169, 14

Burton, W.B. 1992, In *Galactic Interstellar Medium*, eds. Pfenninger, D., Bartholdi, P. (Springer-Verlag), p.1

Deul, E.R. & den Hartog, R.H. 1990, A&A, 229, 362

Elmegreen, B.G., Kim, S., & Staveley-Smith, L. 2001, ApJ, 548, 749

Gott, J. R., Dickinson, M., & Melott, A. L. 1986, ApJ, 306, 341

Gott, J. R., et al. 1990, ApJ, 352, 1

Heiles, C. 1984, ApJS, 55, 585

Kamphuis, J., Sancisi, R., & van der Hulst, T. 1991, A&A, 244, 29

Kim, S., Staveley-Smith, L., Dopita, M.A., Freeman, K.C., Sault, R.J., Kesteven, M.J., & McConnell, D. 1998, ApJ, 503, 674

Kim, S., Dopita, M.A., Staveley-Smith, L., & Bessell, M.S. 1999, AJ, 118, 2797

Kim, S., Staveley-Smith, L., Dopita, M.A., Freeman, K.C., Sault, R.J., Kesteven, M.J., & McConnell, D. 2003, ApJS, 148, 473

Kulkarni, S.R., & Heiles, C. 1988, IN: Galactic and extragalactic radio astronomy (Berlin and New York, Springer-Verlag), pp. 95-153

Lazarian, A., & Pogosyan, D. 2000, ApJ, 537, 720

Lucke, P.B., & Hodge, P.W. 1970, AJ, 75, 171

McKee, C.F., & Ostriker, J.P. 1977, ApJ, 218, 148

Melott, A. L., Cohen, A. P., Hamilton, A. J. S., Gott, J. R., & Weinberg, D. H. 1989, ApJ, 345, 618

Rhode, K.L., Salzer, J.J., Westpfahl, D.J., & Radice, L.A. 1999, AJ, 118, 323

Padoan, P., & Nordlund, A. 2002, ApJ, 576, 870

Park, C., Gott, J. R., & Choi, Y. J. 2001, ApJ, 553, 33

Park, C., Gott, J. R., Melott, A. L., & Karachentsev, I. D. 1992, 387

Puche, D.J., Westpfahl, D., Brinks, E., & Roy, J.-R. 1992, AJ, 103, 1841

Stanimirovic, S., Staveley-Smith, L., Dickey, J.M., Sault, R.J., & Snowden, S.L. 1999, MNRAS, 302, 417

Staveley-Smith, L., Sault, R.J., Hatzidimitriou, D., Kesteven, M.J., & McConnell, D. 1997, MNRAS, 289, 225

Staveley-Smith,?L., Kim,?S., Calabretta,?M.R., Haynes,?R.F., & Kesteven,? M.J. 2003, MNRAS, 339, 87

Thilker, D., Braun, R., & Walterbos, R.A.M. 2000, AJ, 120, 3070

Wada, K., Spaans, M., & Kim, S. 2000, ApJ, 540, 797

Walter, F., & Brinks, E. 2001, AJ, 121, 3026

Wang, Q., & Helfand, D.J. 1991, ApJ, 370, 541

Fig. 1.— The H I brightness temperature map of the LMC (Kim et al. 1998) used in the present work. Superposed are the circles of radii of 700 (outer most), 600, and 500 pixels, where one pixel corresponds 20″ or 5 pc at the distance of the LMC.

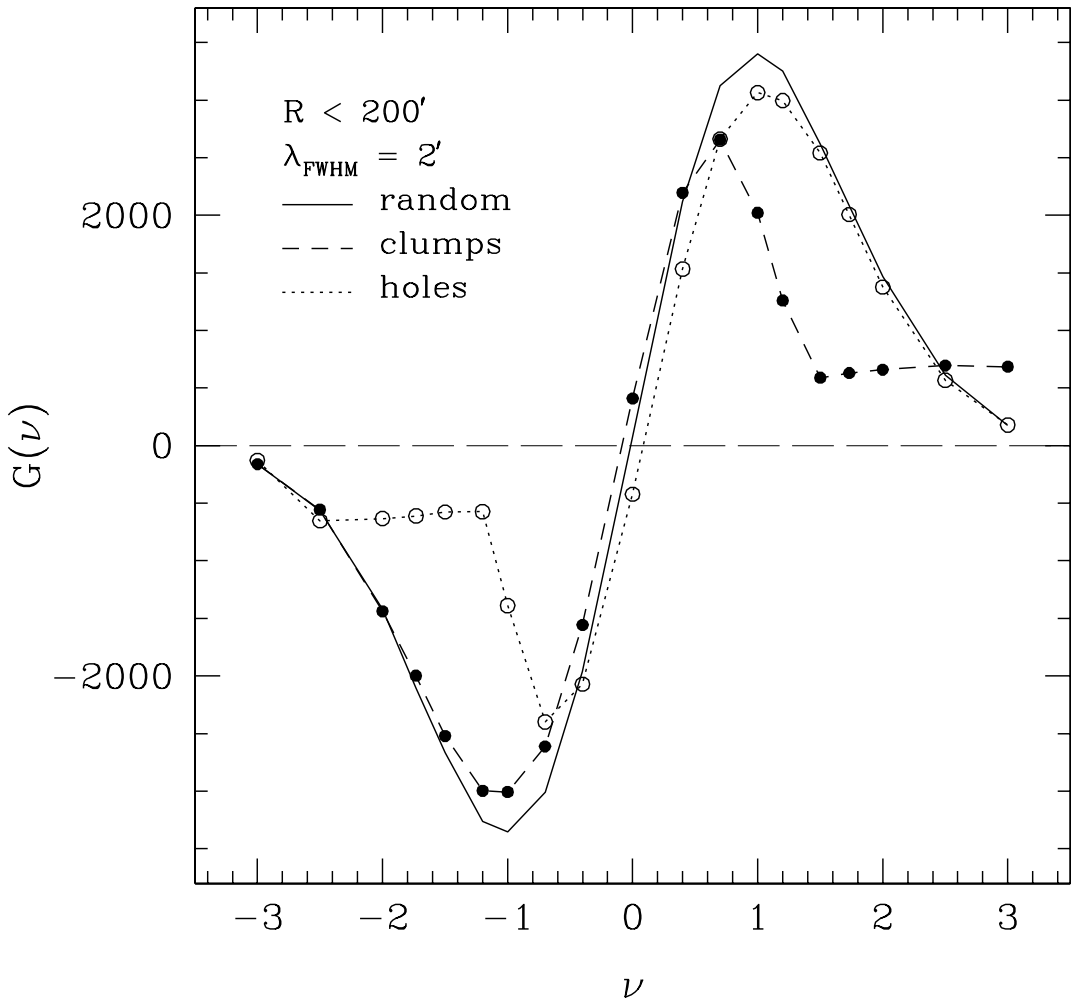

Fig. 2.— Genus curves of three toy models of matter distribution in a circular disk. The solid line is the genus curve of a disk with Poission matter distribution. The dashed line with filled circles is for a disk of Poission matter distribution with additional 857 clumps of diameter of $4'$, and the dotted line with open circles is for a disk with 857 holes of diameter of $4'$ in a Poission matter distribution. The size of the disk is set to 200 arc minutes, and the Gaussian smoothing length is $2'$.

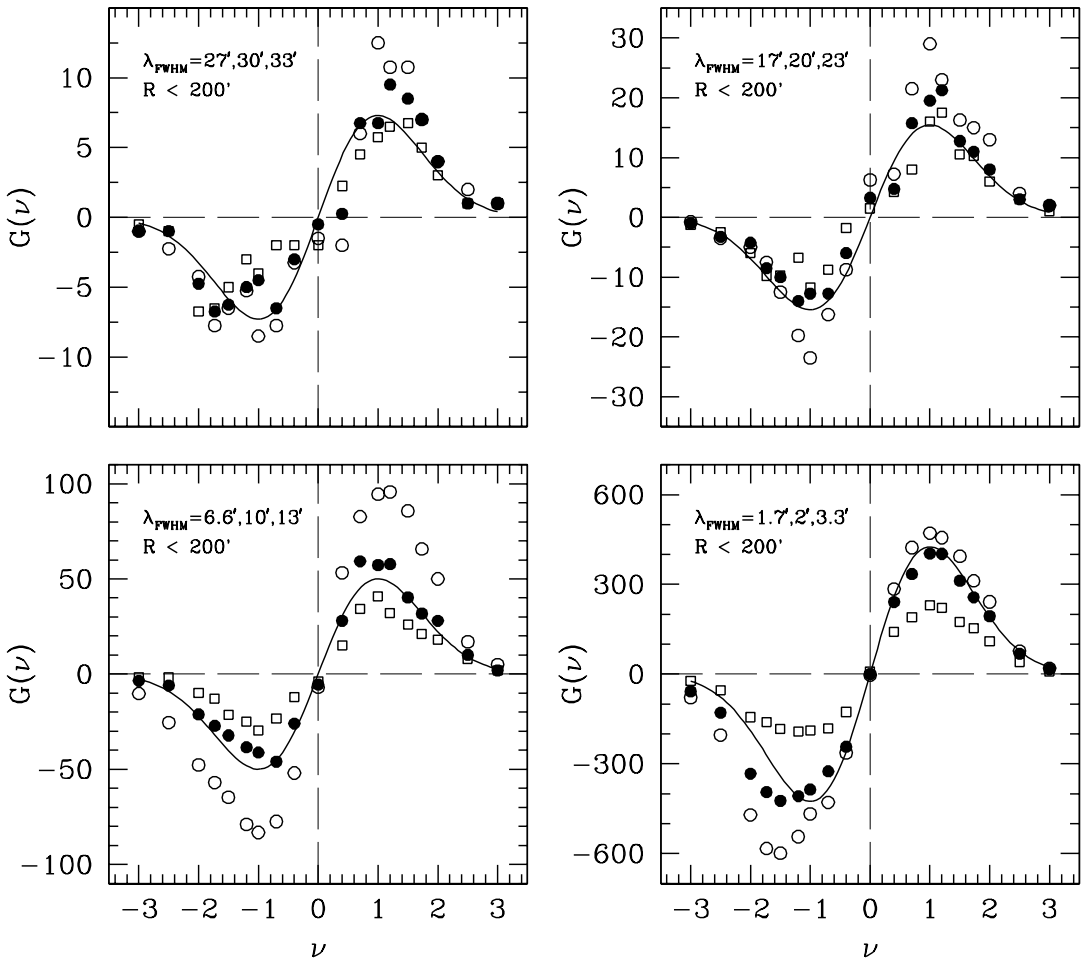

Fig. 3.— The genus curves of the HI map of the LMC at various smoothing scales. The smoothing lengths are in units of pixels and the radius of the circular region under study is set to 200′. In each panel open circles are for the shortest smoothing length, and squares are for the longest smoothing length. The solid line is the Gaussian curve best fitting to the filled circles corresponding to the median smoothing length.

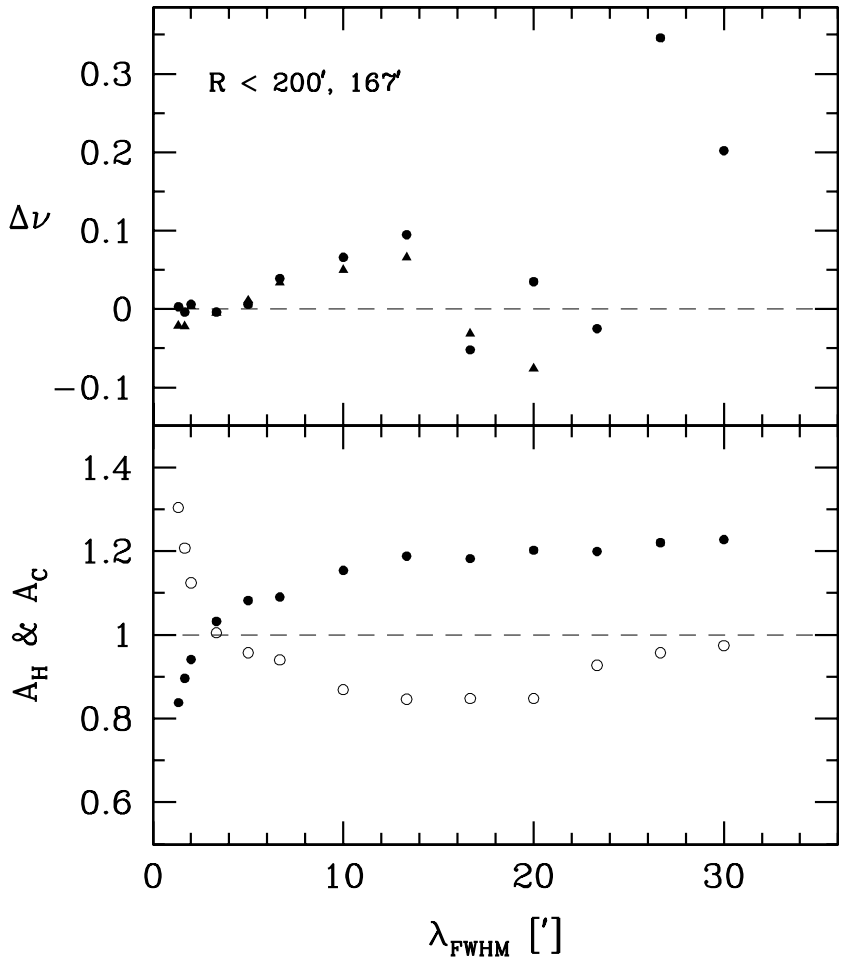

Fig. 4.— Variation of the shift and asymmetry parameters as a function of smoothing length. The circles and triangles in the upper panel are the shift parameters measured from the circular area within radii of $200'$ (or 600 pixels) and $167'$, respectively. In the lower panel the asymmetry parameters A_C (filled circles) and A_H (open circles) are plotted.

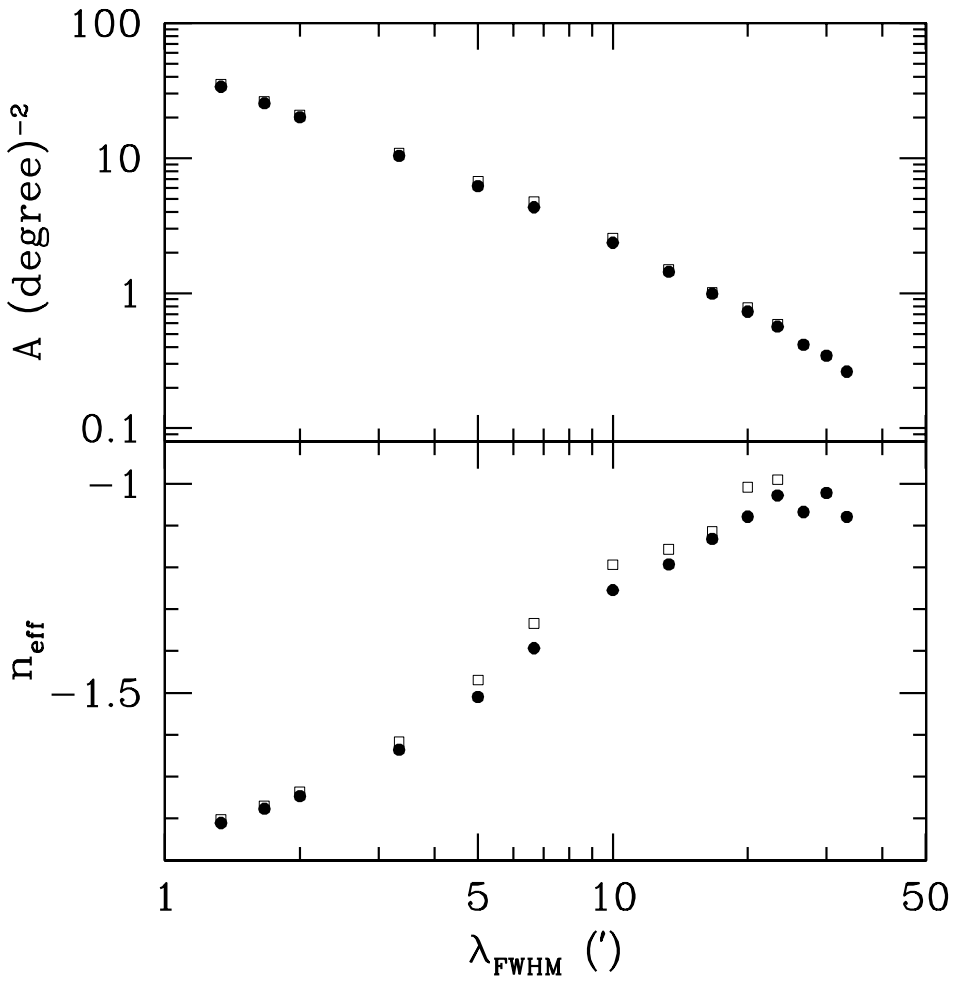

Fig. 5.— (upper) The genus amplitude A per unit square degree as a function of smoothing scale. (lower) The effective power index of the power spectrum of the HI matter fluctuation calculated from the genus density of the upper panel. The filled circles are for the area of radius of 200′, and the open squares are for 167′.